LASER INTERFEROMETER GRAVITATIONAL WAVE OBSERVATORY
- LIGO -
CALIFORNIA INSTITUTE OF TECHNOLOGY
MASSACHUSETTS INSTITUTE OF TECHNOLOGY

Technical Note	**LIGO-T1800238–v1**	2018/08/10

Stabilization of a $2\mu m$ Laser, Interim Report 2

Vinicius Wagner

California Institute of Technology
LIGO Project, MS 18-34
Pasadena, CA 91125
Phone (626) 395-2129
Fax (626) 304-9834
E-mail: info@ligo.caltech.edu

Massachusetts Institute of Technology
LIGO Project, Room NW22-295
Cambridge, MA 02139
Phone (617) 253-4824
Fax (617) 253-7014
E-mail: info@ligo.mit.edu

LIGO Hanford Observatory
Route 10, Mile Marker 2
Richland, WA 99352
Phone (509) 372-8106
Fax (509) 372-8137
E-mail: info@ligo.caltech.edu

LIGO Livingston Observatory
19100 LIGO Lane
Livingston, LA 70754
Phone (225) 686-3100
Fax (225) 686-7189
E-mail: info@ligo.caltech.edu

http://www.ligo.caltech.edu/

1 Introduction and Motivation

The Advanced LIGO interferometers are amongst the most sensitive instruments ever constructed. Even as these observatories progress towards achieving their design sensitivity, work is under way in planning even more sensitive successors [1][2][3]. These will incorporate the the state of the art in materials, control and sensing technology. Key to reaching these improved design sensitivities will be the implementation of cryogenic test masses[1]. These will likely be made from crystalline silicon and will be probed with longer wavelengths in the range of 1550-2000 nm. The choice of $2\mu m$ laser light is a strong candidate wave length given the transparency window of the materials and reduced scatter[4]. Less well known is the performance limitations of lasers of this type and how they might be pre-stablized for use in demanding interferometric experiments.

While NPRO style lasers, previously used at 1064 nm in LIGO, offered inherently narrow line width light, newer fiber coupled technologies such as Discrete-Mode diode lasers are now commercial available at competitive prices. Direct stabilization of these seed laser sources using all fiber assemblies may offer a compact, affordable and low maintenance alternative to more traditional reference cavity pre-stabilization schemes. The characterization of an all fiber stabilized diode laser source will be an important step for delivering $2\mu m$ light to table top experiments used in testing various $2\mu m$ devices for future LIGO use. It will also be an important first step for building a test-bed for assessing the goodness of candidate laser sources for future long wavelength laser interferometers.

Laser stabilization is important for reducing frequency and intensity noise in optic systems. In a system involving a single-frequency laser, there is always noise associated with its output, causing its monochromatic nature to be broadened in its spectral output. Noise in laser sources can originate from a multitude of sources including external acoustic disturbances, internal thermal drift, and spontaneous emission within the laser's gain medium(i.e. quantum noise). Understanding and accounting for these sources is a crucial aspect in obtaining a low noise light source for interferometric experiments. Current LIGO technology uses a 125W laser of 1064nm light and one of the modifications for the LIGO Voyager upgrade is a longer wavelength laser of 2004nm. (This experiment aims to demonstrate all fiber optic stabilization of a relatively noisy (2 MHz linewidth) diode laser source and establish performance limits of such as simple system.)

2 Objectives

The goal of this all-fibered Mach-Zehnder intereferometer(shown in Figure 1) project is to actively stabilize a 2 μm laser and characterize both its *frequency* and *intensity* noise. We will use a path length difference in the intereferometer to make a frequency discriminator and an InGaAs photodiode to measure intensity noise. This project is motivated by the current stage in the LIGO3 PSL Timeline, Noise Characterization and Long-term Stability[1].

To achieve this objective, we will employ a closed loop feedback control system in our set-up to stabilize the frequency of our laser under test. Additionally, we will design an encasement around our intereferometer to passively supress as much thermal and acoustic perturbations

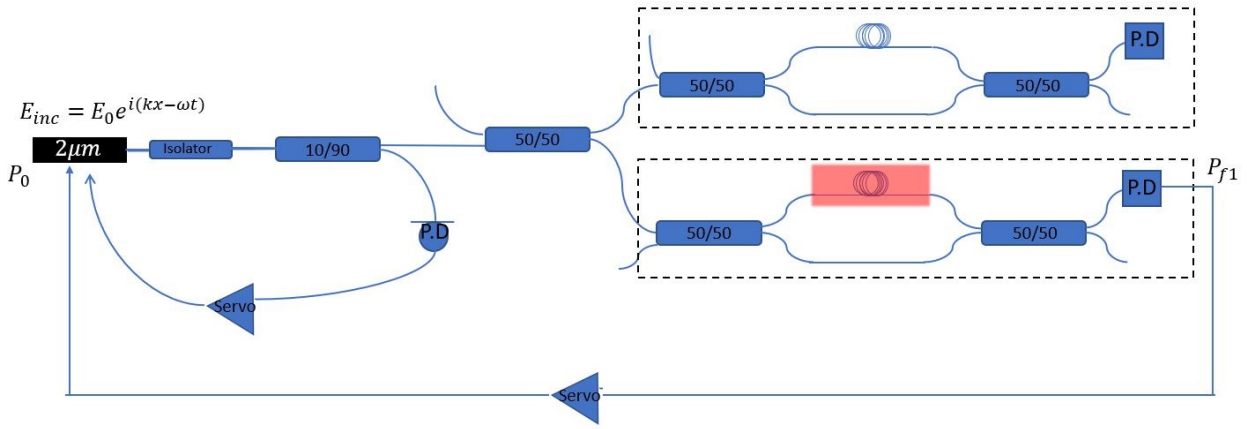

Figure 1: *Experiment set-up, with Mach-Zehnder interferometer delay line and its reference*

as possible. Depending on the progress of the project, we will conclude by investigate the usage of an acousto-optic modulator for intensity noise stabilization. The ideal conclusion of our experiment would be additional data that can support the usage of a longer wavelength laser on the new generation LIGO Voyager.

3 Experiment Approach

Due to the presence of a delay-line in our interferometer, one of the most pressing challenges we initially faced was to calculate the optimal optic fiber length for the arm mismatch. There are various factors that contribute to finding the optimal fiber length such as the power loss throughout the fiber, thermo-optic noise (manifested through the temperature dependance of the fiber's refractive index and linear thermal expansion coefficient), and the fiber's acoustic sensitivity. The underlying matter of this challenge is determining the sensitivity of our interferometer, taking into account the balances between cost and sensitivity losses.

To have a better sense of the ideal sensitivity of our interferometer, we needed to further elaborate on the rough noise budget we had created before the start of the project. With a smaller version (i.e. an interferometer with a shorter length mismatch than desired) of the project already set up, we have begun gathering noise data on the various components used in the set-up, such as our DET10D Photodiode, any required op-amp circuits that we build, and the 2 micron laser itself. Some sources of noise were acquired through manufacturer documentation and simply converted into the equivalent frequency noise (Hz/rtHz), to be added onto our noise budget.

In order to overcome some technical limitations of our experiment's components, or to simply improve their functionality, we have been building our own instrumentation amplifiers. In doing so, we must account for the voltage, resistance, and current noise inherent within these circuits, which are experimentally measured and supplemented by instrument documentation. For instance, in order to translate the current input of our photodiode into

voltage, mainly for the purpose of instrument measurements, we created a transimpedance amplifier(TIA) to be integrated alongside the detector.

4 Progress

4.1 Experiment Housing

To avoid undesired disturbances that could affect our measurements, we housed our experiment in a 17.5x25.5x60.5cm metallic casing with a fiber glass lid. The inner walls are covered with noise-insulating foam padding, as is the table top surface upon which the experiment lies. With the encasing set up, we noticed a significant decrease in the swaying of the intensity in our measurements of the photodetector's power output.

4.2 Characterizing Losses in Optical Components

To have a better understanding of the limitations through our optical components, we measured the power losses through each of them. As expected, particularly in the case of the beam splitters, there are deviations from their 50/50 nature. The output power measured at different locations throughout the experiment are shown below.

Stage-by-stage Power Output		
From Laser through ...	Power (mW) (+/- 0.002mW)	Frequency (Hz)(+/- 3Hz)
Directly from laser	1.339	796.68
Faraday Isolator	0.894	61.09
50/50 Beam Splitter 1 (MZI short arm)	0.528	60.09
50/50 Beam Splitter 1 (Before MZI Long Arm)	0.707	61.20
After Longer arm	1.291	62.30
50/50 Beam splitter 2(Photodiode)	0.762	61.40
50/50 Beam Splitter 2(Beam dump)	0.480	62.30

We can determine the excess power loss, L_p, by considering the total output power from the laser, and the outputs from both ends of the beam splitter under analysis. The following expression is observed:

$$L_p = 10 \log \frac{P_{laser}}{P_1 + P_2}$$

With the data above, we conclude that the excess power loss through Beam Splitter 1 and 2 are 0.351 dB and 0.327 dB, respectively.

4.3 Optimal Path Length

We began with the power loss versus fiber length optimization by considering power at one of our interferometer's outputs, with an attenuation coefficient, α.

$$P_{out} = \frac{P_{in}}{4}(e^{-2\alpha L_1} + e^{-2\alpha L_2} + 2\cos(\frac{2\pi f \Delta L}{c})e^{-2\alpha(L_1+L_2)})$$

Since the ideal scenario for our experiment is to lock the laser's frequency at mid-fringe, we must find where the slope of the output power with respect to the laser's frequency ($\frac{\delta P_{out}}{\delta f}$) is greatest. Taking another derivative of this expression with respect to the long arm length L_2 provides us the sensitivity (S_i) slope of the optic fiber:

$$S_i = \frac{-e^{-\alpha*(L_1+L_2)}\pi P_{in}}{c} + \frac{e^{-\alpha(L_1+L_2)}\pi\alpha\Delta L * P_{in}}{c}$$

The attenuation coefficient was found by referring to the spec sheet of the desired single mode Ge-doped optical fiber by ThorLabs. At a wavelength of 2004nm, the attenuation is given to be roughly $37.5 * 10^{-3} dB/m$ (reference). Finding α is as follows, where β is the given attenuation:

$$10^{\beta x} = e^{\alpha x}$$

$$\beta x * \log 10 = \alpha x \log e$$

$$\alpha = \frac{\beta}{\log e}$$

With the attenuation coefficient of $8.63 * 10^{-2}$, the plot of $\frac{\delta P_{out}^2}{\delta^2 f}$ is shown in Figure 3. Even with a 10 percent sensitivity range reduction, the optimal path length would be around 72 meters, making this optimization too costly. Thus we moved on to explore the inverse relationship given by the optic cable's refractive index dependance on temperature.

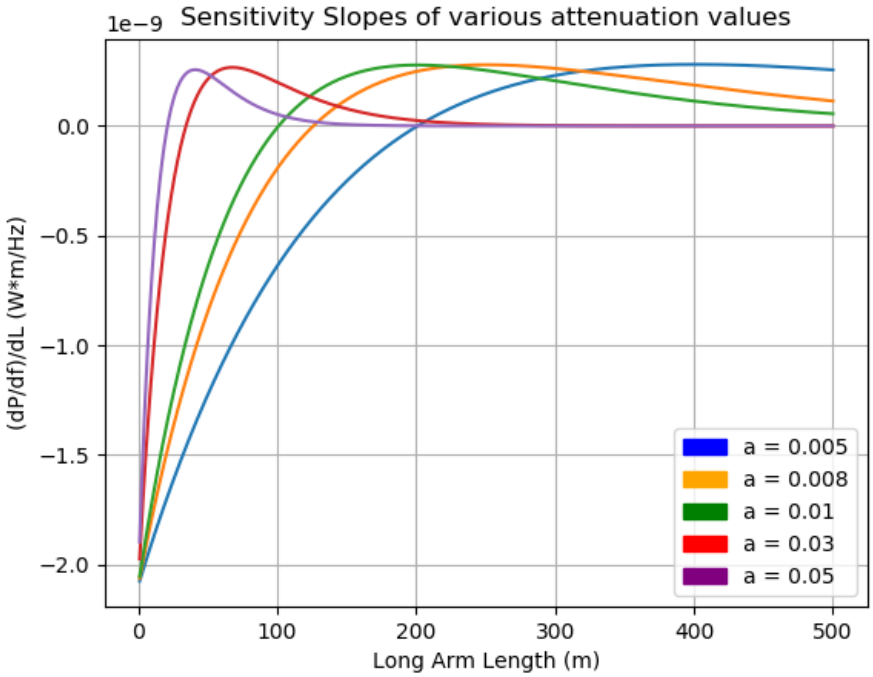

Figure 2: *The sensitivity slope of the fiber optic cable as a function of the long arm length, L_2. The zero point corresponds to the ideal length given some the aforementioned power loss.*

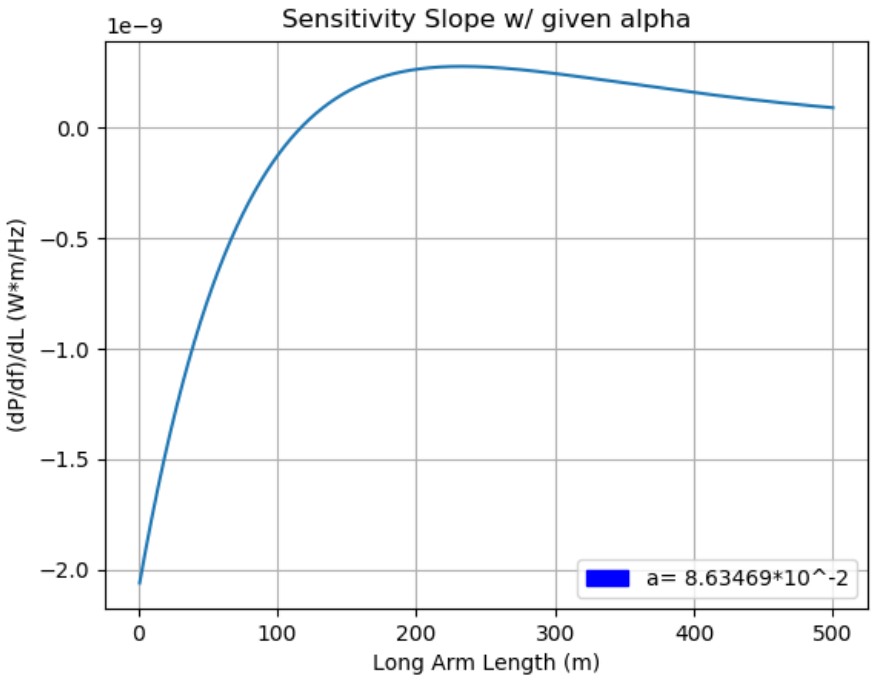

Figure 3: *The sensitivity slope of the fiber optic cable as a function of the long arm length, L_2. The zero point corresponds to the ideal length given some the aforementioned power loss. For this particular $\frac{\alpha}{dB}$ loss, the ideal long arm length lies at roughly 116 meters.*

We are currently in the process of determining the change of refractive index with respect to temperature, $\frac{\delta n}{\delta T}$, which occurs at lower frequencies (50-200Hz). We will go about determining this limiting factor by using the Fluctuation-Dissaption Theorem (FDT) that was used in a previous LIGO report to determine the refractive index and linear expansion dependance on a optic fiber[5][6].

The experiment is currently being set up to have a 10 meter path length difference, which should provide an increase of fringe visibility while not exceedingly suffering the effects of the inherent power loss associated with longer lengths.

4.4 Noise Budget

The aforementioned sources of noise will be represented in an updated noise budget, which we are currently plotting. The previous plot made before the start of the project is show in Figure 4.

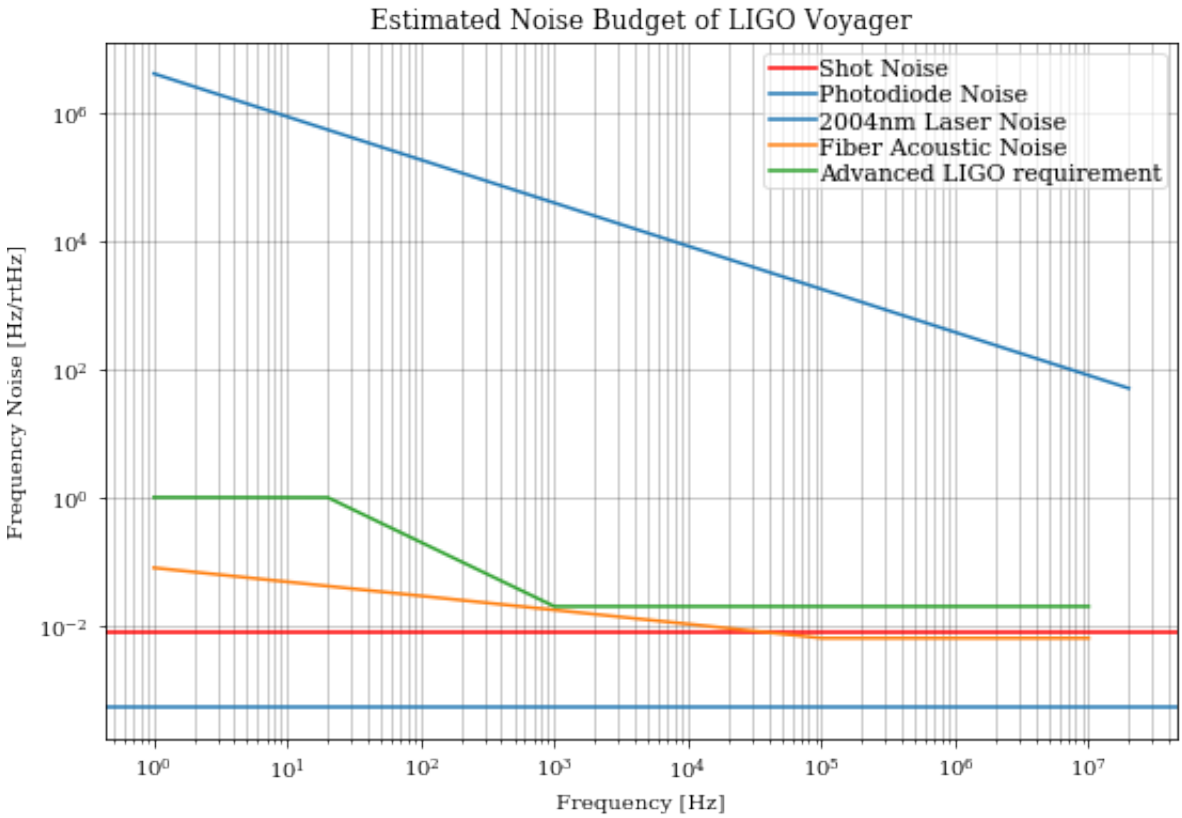

Figure 4: **Noise Budget for LIGO Voyager**, *Shown are the estimated amplitude spectral density of the frequency noise of various sources in the overall set-up. Together they contribute into our system's noise budget, and are compared with the estimated frequency noise requirement of the Voyager 2μm laser, which itself comes from the 1kHz linewidth NPRO frequency noise spectrum scaled by 2000. Based on the laser's wavelength and input power, the shot noise was calculated to be* $2.276 \times 10^{-11}\,\mathrm{W/Hz^{1/2}}$. *From manufacture documentation, the value of the photodiode NEP is* $1.50 \times 10^{-12}\,\mathrm{W/Hz^{1/2}}$. *Assuming a 15m arm length mismatch, the frequency noise equivalent power was calculated to be* $8.144 \times 10^{-3}\,\mathrm{Hz/Hz^{1/2}}$ *and* $5.358 \times 10^{-4}\,\mathrm{Hz/Hz^{1/2}}$ *for the shot noise and photodiode respectively.*

s

4.5 Shot Noise

The shot noise of a photodetector describes its optical intensity noise limit and arises from the discrete nature of electrons and photons, and is a property of a light field[7]. The shot noise of our photodiode can be expressed by the following relationship:

$$\delta n_{sn} = \sqrt{2e^{-}\bar{I}}$$

Where $\bar{I}$ is the average current through the photodiode; gathered from the product of the photodiode's responsivity, approximately $1.2A/W$, and the current reaching the photodiode in our interferometer which we estimate to be roughly $100\mu W$[8]. With this information, it's possible to reach a figure of $6.2 * 10^{-12}A$ for $\bar{I}$. Thus, the shot noise we expect to observe

from our photodiode is $6.2 * 10^{-12}A$. Fortunately, the input referred current for the OP27 ,$0.4\frac{fA}{\sqrt{Hz}}$ at $1kHz$, is lower than this threshold.

4.6 Detector Dark Noise

Dark noise is a current leakage characteristic shared by diodes and arises when a biased voltage is applied in the detector. Upon measuring the dark noise from our DET10D photodiode, we came across the issue that the photodiode was DC biased. This prompted us to develop a simple transimpedance op-amp with the purpose of providing an optimal reading scheme for our measuring instrument and a better signal-to-noise ratio where only the photodiode's shot noise would be the circuit's limiting factor. The schematic is shown in Figure 5. We ran into difficulties in measuring the output signal from the circuit due to a reoccuring oscillations. These oscillations are present due to the large phase margin for the product between the op-amp's gain and feedback factor. Essentially, this is an op-amp phenomena where instability occurs if the rate of the closure between the curves of the gain and reciprocal of the feedback factor approach $40dB$ per decade. To stabilize our TIA, we will need a phase compensation in the form of a bypass capacitor which lies in parallel to the resistor governing the gain of the op-amp. We are currently in the process of this implementation.

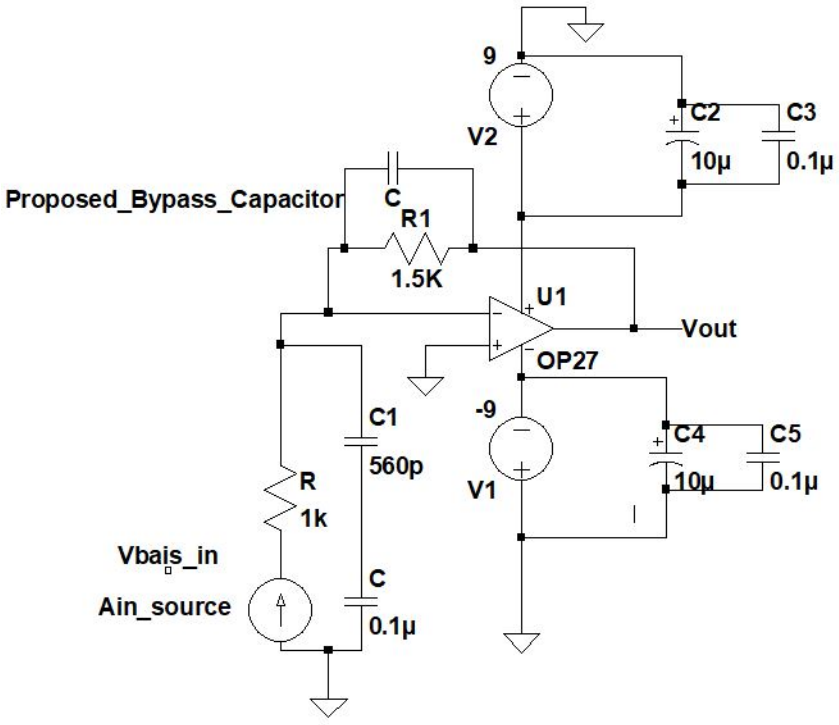

Figure 5: *Schematic for transimpedance op-amp used in conjuction with DET10D photodiode.*

4.7 Acoustic and Thermal Sensitivity

We predict that acoustic noise will be a limiting noise factor in our experiment at lower frequencies, thus having a grounded notion of the sensitivity of our optic fiber is crucial when considering a possible length to purchase. The fiber's sensitivity to some pressure

depends on its characteristic elastic coefficients (Young's Modulus, E, and Poisson's Ratio, σ) and Pockels coefficients, P_{12} and P_{44} [9]. Previous work has been done to calculate these coefficients for pure silica, the material found within the core and part of the cladding of our optic fiber. In an idealized state, our optic fiber can be treated as a cylinder of pure silica. Referenced work measured the pressure acting on the material from variations of the relative phase change between two interferometer arms- one static and the other undergoing a pressure difference relative to it. The optical phase retardation per unit of pressure can be expressed as,

$$\frac{\Delta\phi}{\phi} = \frac{(1-2\sigma)}{E}(\frac{n^2}{2}(3P_{12}+2P_{44}))$$

Following this idealized scenario, the acoustic sensitivity comes out to be $-1.23{*}10^{-14} dyn/cm^2$. We are currently reviewing the scientific precedence on calculating the acoustic sensitivity of a multilayered "cylinder", essentially replicating our optic fiber, which takes into account the varying refractive indices and radial/axial strains[10].

Since measuring the inherent acoustic sensitivity of the experiment's optical fibers material may prove to extend passed the reach of our schedule, we're in the process of adding a microphone along with a piezo-buzzer within the housing of the experiment. This will allow us to experimentally measure the degree of sensitivity of the optical fiber, when compared to a normal lab volume conditions.

Finally, we have created a thermal sensor circuit which will be deployed within and directly outside the experiment's casing to measure environmental temperature variations. Running the circuit through a noise analysis, we find the voltage noise to be on the order of $17.28 \times 10^{-9}\,\mathrm{V/Hz^{1/2}}$ at 10 Hz. In designing the circuit, we took special care in minimizing thermally induced offset drift. Considering our signal is around 7 V, we'd expect to observe around $7.8 \times 10^{-5}\,\mathrm{K}$ of input referred drift per degree Kelvin of drift in the OP27 used.

4.8 Locking and Stabilization

The process of locking and stabilizing the $2\mu m$ laser involves setting up the experiment as a closed feedback loop. Upon first measurement of the photodetector signal with the laser off, we noticed a DC offset of about $22.4 \times 10^{-3}\,\mathrm{V}$, whose cause we are still determining. The next steps take into account this offset. The next step involves finding the mid-fringe point of the photodetector output with the laser turned on, which we determined to be $440 \times 10^{-3}\,\mathrm{V}$ above the offset. We then subtract a voltage reference with an identical value from the PD output to produce an error signal, which is subsequently fed back to the laser diode's current controller, completing the feedback loop. We utillize two daisy-chained pre-amplifiers as the gain element in the feedback loop, with one having a high-pass filter of 1 Hz and 6 dB rolloff and the other DC coupled. Upon DC coupling the two pre-amplifiers and increasing the gain, we expected a linearization of the error signal but instead observed it scanning through a large quantity of fringes, which also caused the laser diode current controller to drastically fluctuate in current value. These characteristics indicate an imperfection in the feedback loop architecture, which we are currently improving.

5 Project timeline and Outlook

Below is the estimated timeline of this 2μm laser stabilization project. At the time of this report, we are in Week 7, Experiment Optimzations and Data Acquisition. We have reached a point where the locking of the laser is underway, and measurements and optimizations are being made. As we progress through the experiment, however, an accurate stabilization scheme may prove to be out of the scope of the 10-week project.

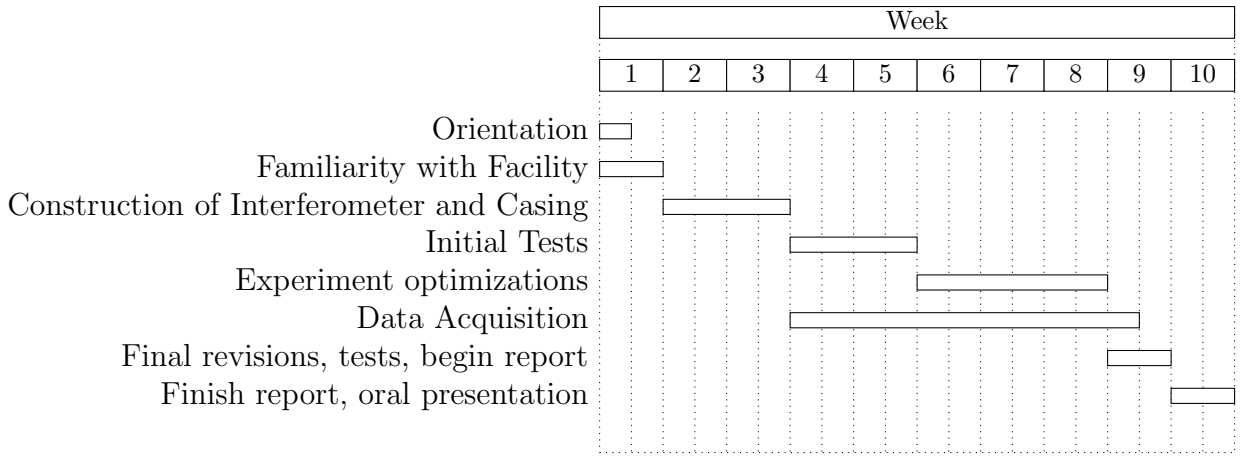

References

[1] Adhikari, Rana X, et. al, *LIGO Voyager Upgrade: Design Concept*. LIGO Scientific Collaboration, LIGO-T1400226-v9 (2014)

[2] Hild, Stefan, et. al, *Pushing towards the ET sensitivity using "conventional" technology*. School of Physics and Astronomy at University of Birmingham, Issue 2 (2014)

[3] LIGO Scientific Collaboration, *Instrument Science White Paper*. LIGO Scientific Collaboration, LIGO-T15TBIv1 (2014)

[4] Edward, Taylor and Smith-Lefebvre, Nicolas, *Quality Factor of Crystalline Silicon at Cryogenic Temperatures*. LIGO Scientific Collaboration (2013)

[5] Conant, Emily; Hall, Evan; Adhikari, Rana; Chalermsongsak, Tara, *Transportation of Ultra-Stable Light via Optical Fiber*. LIGO Scientific Collaboration, T1400501-v1 (2014)

[6] Callen B., Herbert and Welton A., Theodore, *Irreversibility and Generalized Noise*. Randal Morgan Laboratory of Physics, University of Pennsylvania (1951)

[7] Richardson, W. H., et. al, *Squeezed Photon-Number Noise and Sub-Poissonian Electrical Partition Noise in a Semiconductor Laser*. NTT Basic Research Laboratories(1991)

[8] ThorLabs, *DET10D(/M) Extended InGaAs Biased Detector, User Guide* (2017)

[9] N. Lagakos, et. al, *Acoustic sensitivity predictions of single-mode optical fibers using Brillouin scattering*. Applied Optics, Vol. 19, No. 21 (1980)

[10] Hughes, R. and Jarzynski, J., *Static pressure sensitivity amplification in interferometric fiber-optic hydrophones*. Applied Optics, Vol. 19, No. 21 (1980)